IOPscience iopscience.iop.org

Home Search Collections Journals About Contact us My IOPscience

Structural features and phase transition temperature of $Ba_xSr_{1-x}TiO_3$ films grown on various substrates

This article has been downloaded from IOPscience. Please scroll down to see the full text article.

2002 J. Phys.: Condens. Matter 14 6823

(http://iopscience.iop.org/0953-8984/14/27/306)

View the table of contents for this issue, or go to the journal homepage for more

Download details:
IP Address: 171.66.16.96
The article was downloaded on 18/05/2010 at 12:14

Please note that terms and conditions apply.

INSTITUTE OF PHYSICS PUBLISHING JOURNAL OF PHYSICS: CONDENSED MATTER

J. Phys.: Condens. Matter **14** (2002) 6823–6831 PII: S0953-8984(02)34655-1

Structural features and phase transition temperature of $Ba_xSr_{1-x}TiO_3$ films grown on various substrates

S F Karmanenko[1], **A I Dedyk**[1], **A A Melkov**[1], **R N Il'in**[1], **V I Sakharov**[2], **I T Serenkov**[2] **and Jowoong Ha**[3]

[1] State Electrotechnical University, St Petersburg, 197376, Russia
[2] Ioffe Physico-Technical Institute, St Petersburg, 194026, Russia
[3] 'Inostek Inc' Keumchum Gasan, Seoul, 356-1, Korea

Received 7 March 2002
Published 28 June 2002
Online at stacks.iop.org/JPhysCM/14/6823

Abstract
Ferroelectric $Ba_xSr_{1-x}TiO_3$ (BSTO) films were grown on various substrates (α-Al_2O_3, $LaAlO_3$, MgO and polycrystalline alumina) by RF sputtering of a BSTO target with Ba/Sr ratio x in the range from 0.50 to 0.65. The results of comprehensive structural diagnostics of the films are correlated with the temperature T_m corresponding to the maximum capacitance of a planar BSTO varactor, measured at a frequency of 1 MHz. BSTO films of the same cationic composition, grown on various single-crystal substrates, have markedly different T_m correlated with the structural ordering of ferroelectric films. Highly oriented $BaSrTiO_3$ films approximately 300 nm thick, grown on MgO and $LaAlO_3$ substrates, are characterized by low $\tan\delta \leqslant 8 \times 10^{-4}$ and $T_m = 140-230$ K. However, textured and polycrystalline BSTO films of the same composition, grown on sapphire and alumina substrates, are less strained, having $\tan\delta \leqslant 10^{-3}$, and $T_m > 250$ K.

1. Introduction

The fast development of microwave electronics needs high-quality tunable components for communication and navigation systems, and ferroelectric films (FEF) show considerable potential in this regard [1–3]. In the ferroelectric material, the phase transition from the paraelectric to the ferroelectric phase occurs at the Curie temperature T_c corresponding to the maximum relative permitting ε. This temperature is determined by the composition of a ferroelectric compound. At present, the perovskite solid solution $Ba_xSr_{1-x}TiO_3$ (BSTO) is the most appropriate, among ferroelectric compounds, for microwave applications [3, 4]. Oriented BSTO samples are characterized by the presence of microdeformation and built-in electric fields that shift T_c from the equilibrium value. Therefore, in real strained ferroelectric samples there is some difference between T_c and T_m—the temperature corresponding to the maximum of the $\varepsilon(T)$ dependence. The phase transition temperature and dielectric response

 © 2002 IOP Publishing Ltd Printed in the UK

of FEF are affected by many factors, such as crystal perfection, oxygen deficiency, grain size, microdeformations, charged states and substrate properties. A model approach describing the $\varepsilon(T)$ dependence and the dielectric characteristics of FEF was successfully demonstrated in [5], however, some important physical factors were disregarded. In the present study, we examined the influence exerted by the structural quality and microdeformations in the films on the dielectric characteristics and the T_m parameter of BSTO films grown on various substrates suitable for microwave electronics.

2. Film preparation

The following substrates: MgO (100), $LaAlO_3$ (100) (henceforth LAO), sapphire— α-Al_2O_3 (r-cut $[10\bar{1}2]$) (designated as α) and alumina (alum) were used. The mismatch factor was defined as follows: $\xi = 2(a_S - a_F)/(a_S + a_F)$, where a_S, a_F are the lattice parameters of the substrate and film, respectively. Thus, for $BaSrTiO_3$ films: $\xi(\alpha) \approx 18-26\%$; $\xi(\text{MgO}) \approx 6\%$; $\xi(\text{LAO}) \approx -3.7\%$ [6]. Rhombic distortions of the sapphire surface led to stronger mismatch. The thermal expansion coefficients (β) and the chemical activity at the interface are also to be taken into account. The β coefficient increases in the following order: MgO $<$ LAO $<$ BSTO $< \alpha$. The BSTO/LAO structure is characterized by the closest β values. Other FEF/substrate structures have β(BSTO)/$\beta(\alpha)$ and β(BSTO)/β(MgO) ratios of about 1.5.

The films were grown under the following conditions: oxygen pressure during sputtering 10–80 Pa; film-to-substrate distance 15–50 mm; composition of the $Ba_xSr_{1-x}TiO_3$ powder target $x = 0.50-0.65$; specific RF discharge power 6–10 W cm^{-2}; substrate temperature 650–750 °C; film growth rate 1.5–2 nm/min (see also [7]). A study of the initial stage of BSTO film formation showed that epitaxial growth occurs only on LAO and MgO substrates, although the nucleation mode is strongly dependent on the preparation mode. At substrate temperatures higher than 700 °C and high enough oxygen pressure (no less than 20 Pa) we detected growth of highly oriented films on both types of substrate.

3. Film structure diagnostics

The FEF structure was studied by the following techniques: x-ray diffraction (XRD), medium-energy ion scattering (MEIS), scanning electron microscopy (SEM) and transmission electron microscopy (TEM). An XRD analysis of BSTO/MgO, BSTO /α and BSTO/LAO structures characterized the crystal orientation, and microstrains ($\Delta a/a$). The films grown in a single preparation cycle were free from impurity phases and their XRD patterns displayed (k00) modes only. Figure 1 shows XRD patterns of BSTO films on various substrates (sapphire, LAO and MgO) grown in a single run. The diffraction patterns presented in figure 1 reveal highly oriented film structure alongside with some difference in crystal lattice parameter. The ($\tan\delta$) ratio found from the diffraction patterns is presented in table 1. The highest ($\Delta a/a$) parameter ($\sim 5 \times 10^{-3}$) was obtained for BSTO/LAO structures.

Detailed information concerning the film structure and lattice quality was obtained by MEIS diagnostics described earlier [8, 9] for the example of perovskite films. The MEIS diagnostics used ions with energy of 180–250 keV, because it had better depth resolution than the traditional Rutherford backscattering technique [9]. By fitting simulated backscattered-ion energy spectra to the experimental ones, the film thickness and composition were determined. For this purpose, we compared the film spectra with the spectra of homogeneous $SrTiO_3$ and $BaTiO_3$ single crystals. The film thickness was measured in number-of-atoms-per-square-

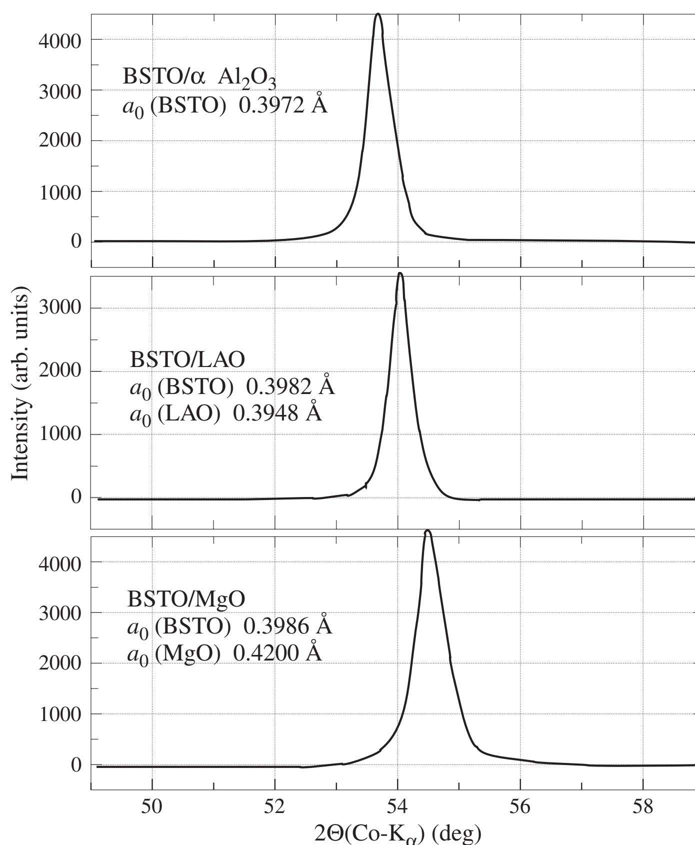

Figure 1. X-ray diffraction patterns of BSTO films grown on various substrates (sapphire, LAO, MgO) in a single run.

centimetre units and was converted to nanometres on the assumption that the $BaSrTiO_3$ crystal density is 5.64 g cm^{-3}.

Ion channelling was applied to perform structural analysis. The intensities of backscattered ions were measured in relation to their energies for the channelling (aligned) $Y_c(E)$ and random $Y_r(E)$ modes. With a knowledge of the stopping power and backscattering cross sections, these energy dependences $Y(E)$ can be transformed into those on thickness, $Y(t)$. The ratio $Y_c(E)/Y_r(E) = \chi(E)$ is the relative ion dechannelling yield and the value of $\chi(E)$ just after the surface peak is the minimum yield χ_0. The $\chi(t)$ dependence for the films can be described by the empirical formula:

$$1 - \chi(t) = (1 - \chi_0)\exp\left(-\frac{t}{\lambda}\right) \tag{1}$$

where λ is the dechannelling length. Such a relation, corresponding to uniform concentration of extended defects in a film, was proposed in [10]. We studied by the MEIS method BSTO films deposited onto (100) MgO, (100) $LaAlO_3$ and R-cut (1102) Al_2O_3 single-crystal substrates. The backscattering spectra for random and aligned directions and the $\chi(E)$ dependences are given in figures 2 and 3.

Table 1. Parameters of BSTO films.

	Substrates							
Parameters	MgO	LAO	α	LAO	α	LAO	α	alum
Sample number	1	2	3	4	5	6	7	8
Film thickness (nm)	650	650	650	750	750	650	650	650
$Ba_xSr_{1-x}TiO_3$ target x	0.60	0.60	0.60	0.53	0.53	0.55	0.55	0.55
Gas composition	Ar/O_2	Ar/O_2	Ar/O_2	O_2	O_2	O_2	O_2	O_2
Pressure (P)	20	20	20	20	20	40	40	40
Temperature T_s (°C)	750	750	750	700	700	650	650	650
Lattice parameter, a_0 (Å)								
film	3.968	3.985	3.962	3.9775	3.958	3.9775	3.958	3.960
bulk material	3.964	3.964	3.964	3.958	3.958	3.961	3.961	3.961
Microstrains $\Delta a/a$ (10^{-4})	10	52	5	50	0	40	75	−2.5
Temperature of ε maximum, T_m (K)	180	230	330	140	260	140	262	257
ε (300 K)	1330	2400	2100	2500	1900	2450	1900	1800
$\tan\delta$ (300 K) $\times 10^{-4}$	4	9	15	6	19	5	12	15
T (300 K)	1.25	1.45	1.90	1.1	2.4	1.1	2.4	2.1

The minimum ion yield for a 180 nm thick BSTO film grown on a MgO substrate is rather low, $\chi_0 \approx 0.03$. This value is close to that calculated for a perfect single crystal. The $\chi_0(E)$ value is slowly increased with the film depth enhancement. The low-energy part of the spectrum in figure 2 belongs to the substrate and is clearly separated from the film-related part. The dependence $\chi_0(E)$ shows a maximum near the film/substrate interface. Misfit dislocations accumulated in the interfacial region of film are responsible for this maximum. The previously estimated surface concentration of misfit dislocations is approximately 1.5×10^6 cm^{-1} [11]. In this case, the obtained $\chi_0(E)$ dependence suggests that the film microdeformations caused by the lattice mismatch are relaxed only through misfit dislocations, and upper layers of the film grow in the layer-by-layer mode. The dechannelling across the BSTO film profile is characterized by $\lambda = 1.7 \times 10^{19}$ atom cm^{-2}.

The lattice mismatch for BSTO and LAO single crystals is less than that in the BSTO/MgO case, but, at temperatures lower than 435 °C, the LAO lattice has small rhombohedral distortions. The MEIS spectrum for a 380 nm thick BSTO film grown on LAO substrate is presented in figure 3(a). The minimum yield $\chi_0 = 0.32$ is higher and the $\chi_0(E)$ dependence increases faster ($\lambda = 3.2 \times 10^{18}$ atom cm^{-2}) than that for BSTO/MgO structure. The fast increase indicates on high defect concentration between the surface and film/substrate interface. In the interfacial region, the dependence $\chi(E)$ has a bend caused by ion beam transition from the defective film into the single-crystal substrate. The maximum in this region is inconspicuous owing to the low concentration of misfit dislocations. Apparently, in the BSTO film deposited on LAO substrate the strains are relaxed via formation of extended defects in the film bulk.

The BSTO film deposited on the r-plane of sapphire substrate is characterized by lattice mismatch $\xi > 0.2$ and essential rhombic distortions. That is why the channelling is weak or absent in this case. The spectrum for a 170 nm thick BSTO film deposited on the r-plane of sapphire is given in figure 3(b). The high value of $\chi_0 = 0.8$ is accounted for defects, such as grain boundaries detected by SEM, and by the polycrystalline structure revealed by TEM. The bend of the $\chi(E)$ dependence in the interfacial region is caused by the difference between the normal to the r-plane of sapphire surface and the channelling direction in the r-cut sapphire. The minimum yield χ for thicker films may be as high as 100%.

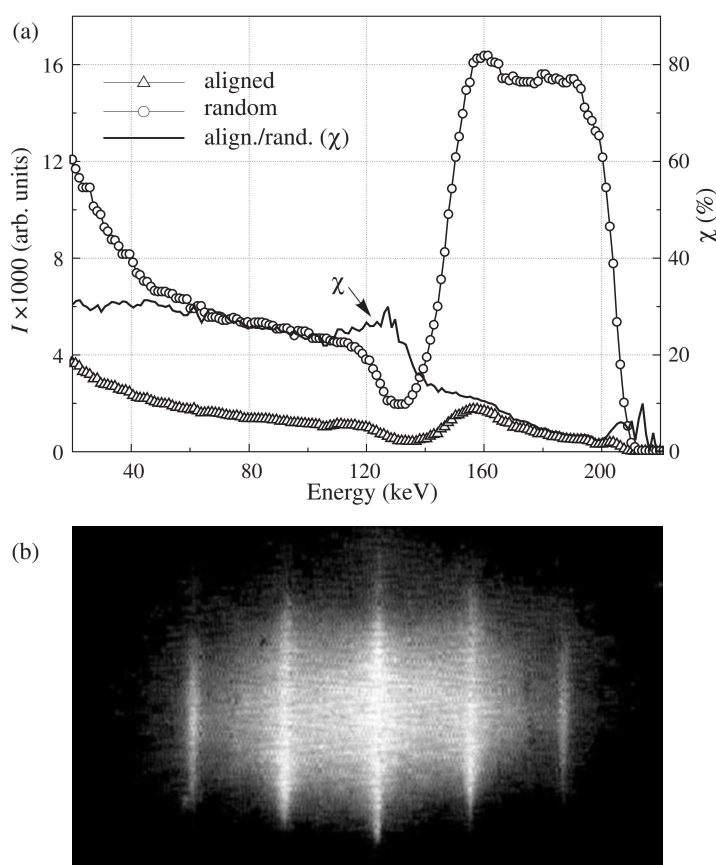

Figure 2. Structural characterization of BSTO film grown on MgO substrate. (a) Medium energy ion back scattering spectra for random and aligned directions and $\chi(E)$ dependence; (b) reflection high energy electron diffraction pattern of the same BSTO/MgO structure.

Thus, an increase in the film thickness t leads to larger χ parameter. For a 800 nm thick BSTO/LAO film, $\chi_0 \approx 50\%$ and a BSTO/α structure with the same FEF thickness is characterized by relative yield near the film surface, $\chi_S \approx 100\%$. BSTO films grown on sapphire substrates have highly-oriented structure, although the ion channelling is rather weak. Figure 4 presents surface micrographs of the investigated films. These images were obtained by SEM on planar capacitor structures patterned from a Cu/BSTO structure by photolithography and chemical etching. The electrodes enabled a SEM study of the BSTO films owing to the drain of charge concentrated on a dielectric film. One can see the difference between the surface morphologies of BSTO films grown on LAO and sapphire substrates. The smoothest surface and homogeneous structure are revealed in BSTO films grown on LAO (or NGO) substrates. The films prepared on sapphire show clear grain boundaries of crystallites with average grain size of about 300 nm.

The features of the BSTO film structure were confirmed by TEM investigations. TEM images and diffraction patterns of BSTO films grown on LAO and α substrates are presented in figure 5. One can see large blocks in the BSTO/LAO sample and the polycrystalline structure of the BSTO/α films. The films grown on sapphire substrates have well-pronounced [001] texture confirmed by high-energy electron diffraction (see figure 5(a)).

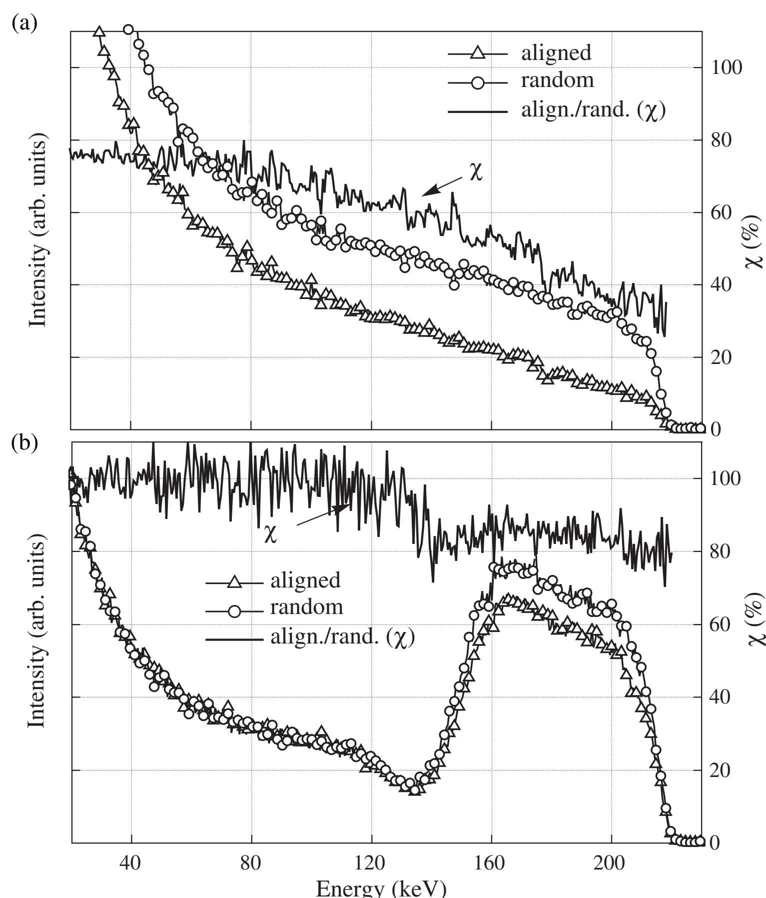

Figure 3. MEIBS spectra of BSTO films grown on LAO (a) and sapphire (b) substrates. The spectra were obtained using 230-keV H^+ ion beam.

4. Dielectric parameters

The dielectric properties of BSTO films were studied on planar capacitors—varactors with Cu electrodes with $w = 4-15\,\mu$m interelectrode spacing. The relative permittivity ε and the dielectric loss tangent $\tan\delta$ were calculated from the varactor capacitance, reactance and conductivity measured at a frequency of 1 MHz and voltage amplitude of 0.1 V. To determine ε, we used the known equation presented, e.g., in [3]. The temperature dependences of $C(T)$ and $\tan\delta(T)$ were studied in the range 77–420 K. The tunability of ferroelectric varactors under the action of static electric field was determined from capacitance–voltage characteristics $C(U)$ measured in electric fields of up to 50 V μm^{-1}. Thus, we evaluated such parameters as the tunability factor $T = [C_0 - C(U_{\max})]/C(U_{\max})$ and the hysteresis $\eta = C_0 - C(0)/C_0$ of the capacitance–voltage characteristics. The capacitance C_0 is the initial value, and $C(0)$ is the capacitance in zero electric field on applying a bias voltage cycle. The dielectric characteristics of FEF deposited on different substrates are given in table 1. It can be seen that BSTO films on MgO and LAO substrates have T_m between 140 and 230 K, $\tan\delta$ in the range from 4×10^{-4} to 9×10^{-4} and $\Delta a/a > 10^{-3}$. The highest ε value is observed for the BSTO/LAO structure.

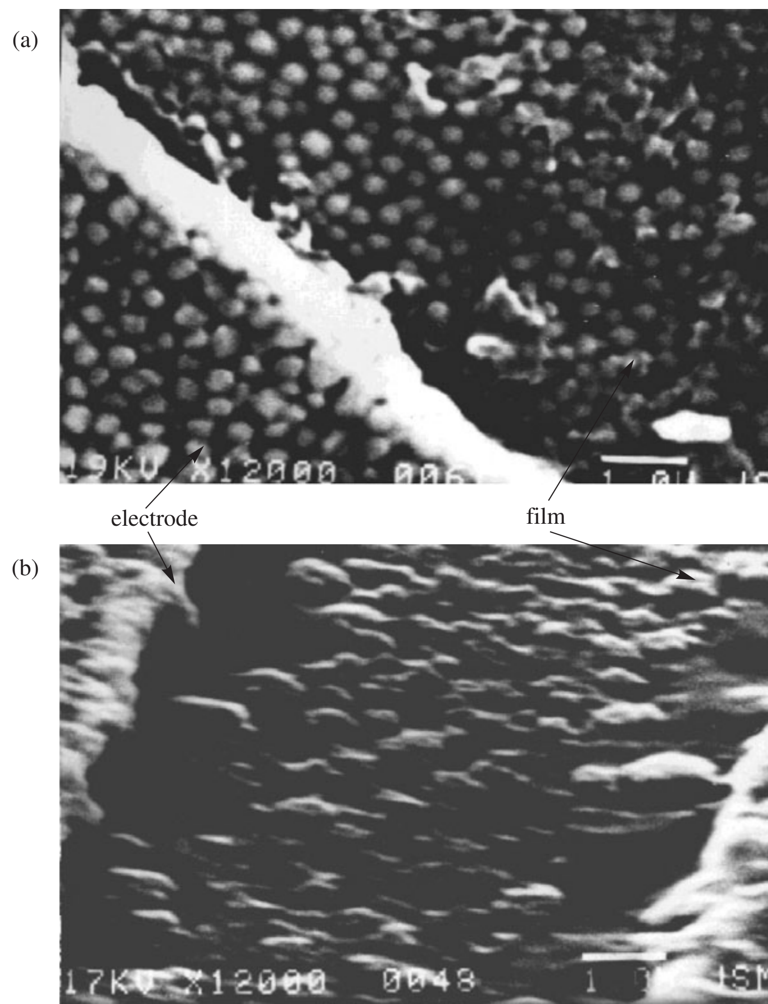

Figure 4. Morphology of BSTO films grown in the same run on the following substrates: (a) LAO (No 6, see the table); (b) sapphire α-Al_2O_3 {1012} (No 7). The SEM images were obtained in the gap of planar capacitors with Cu-electrodes.

For the films deposited on α and alumina substrates the T_m value varies between 260 and 330 K, $\tan\delta$ ranges from 15×10^{-4} to 19×10^{-4} and $\Delta a/a < 5 \times 10^{-4}$.

Figure 6 shows the dependence of $\tan\delta$ on film thickness for BSTO/α and BSTO/LAO structures prepared at oxygen pressure of ~20 Pa. The lowest dielectric losses were obtained on 500–600 nm thick films. Probably, a certain decline in dielectric losses with increasing film thickness t is due to the development of an extended network of defects and block boundaries. The increase in $\tan\delta$ in BSTO/LAO structures reflects a deterioration of the epitaxial growth mechanism, starting from film thickness of approximately 300 nm. Comparing the parameter deviations for a preparation route, we can conclude that the lattice parameter affects most strongly the maximum in the $\varepsilon(T)$ dependence. This conclusion is in agreement with the results of [12], where the crucial role of lattice distortions on the dielectric losses and microwave quality factor was outlined. Our experiments show that lattice distortions are mostly responsible for the considerable deviations of the T_m parameter.

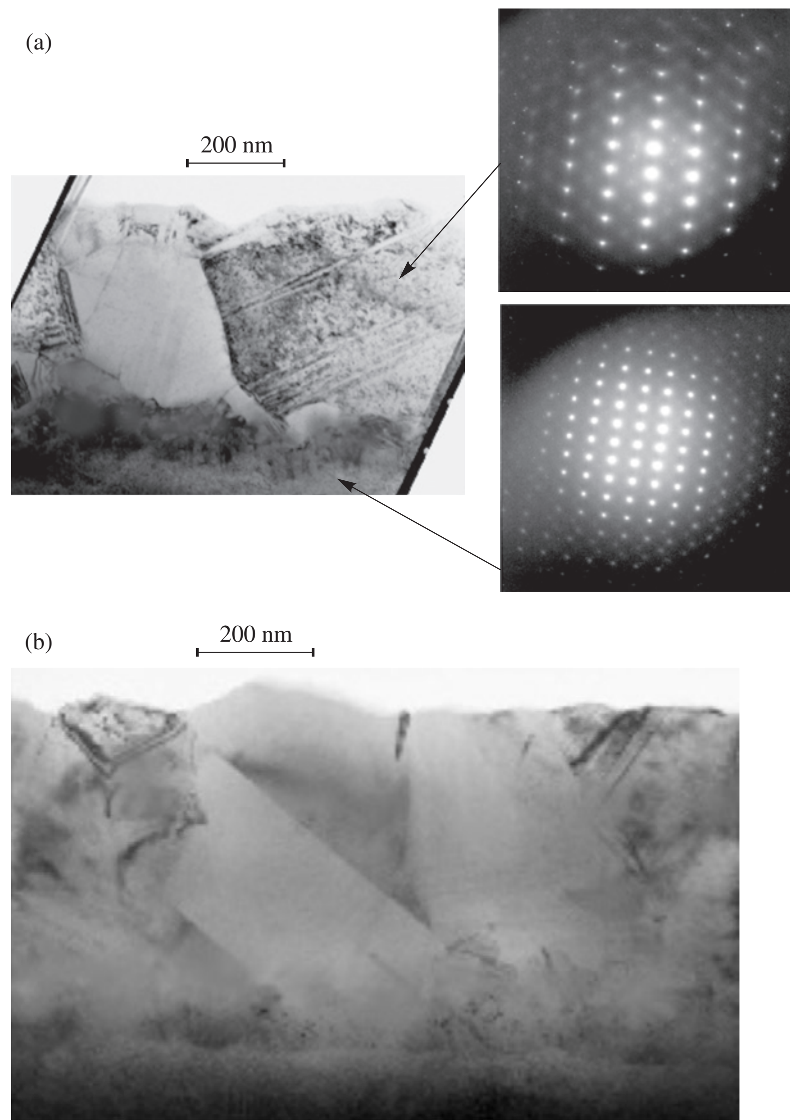

Figure 5. TEM images and diffraction patterns of BSTO films. (a) film grown on LAO substrate; (b) film grown on α-substrate.

Figure 7 presents the dependences of T_m on the oxygen pressure in film deposition. The technological factor $P(O_2)$ affects the concentration of oxygen vacancies in the perovskite lattice. Hence it follows that the decrease in $[V_0]$ in the BSTO crystal lattice suppresses cell distortions and leads to smaller difference in T_m between the BSTO/LAO and BSTO/α structures. In order to explain the experimental temperature dependences of the relative permittivity and to model their behaviour, we used a phenomenological description [5]. We suggest that FEFs consist of sublayers with varied x parameter in the $Ba_xSr_{1-x}TiO_3$ compound. The model considerations in [12] provide a good explanation for the experimental $C(T)$ and $\varepsilon(T)$ dependences.

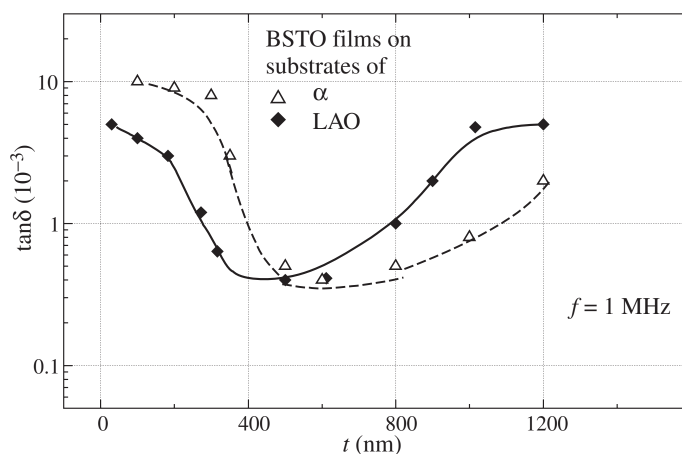

Figure 6. Dependence of tan δ on film thickness of BSTO/α and BSTO/LAO structures prepared at oxygen pressure ~20 Pa.

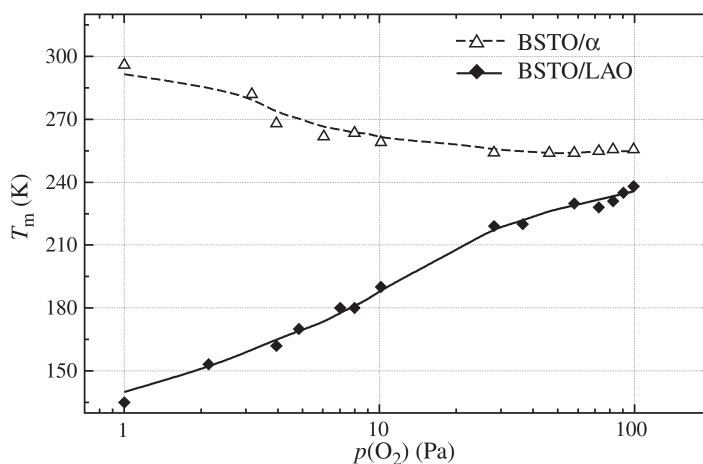

Figure 7. Dependences of T_m parameter corresponding to the maximum value of relative permittivity on oxygen pressure in the process of film deposition.

5. Conclusion

The structural characteristics of FEF, obtained by MEIS, XRD, TEM and SEM methods, combined with the results of dielectric measurements, made it possible to reveal some features of BSTO films deposited on different substrates. The BSTO films grown on MgO substrates are distinguished by high crystal quality despite the essential lattice mismatch. The BSTO/MgO films show epitaxial structure and lowest relative ion yield ($\chi_0 \approx 0.02$). However, the crystal structure of BSTO films grown on MgO is characterized by the strongest microdeformations manifested in a shift of the XRD reflections and the T_m value. The difference in T_m between BSTO/MgO films and polycrystalline ceramic samples of the same component composition is more than 100 K. A similar situation is observed for the case of BSTO/LAO structure, although the crystal quality of this kind of films is not so high as that for BSTO/MgO.

Both the BSTO/MgO and BSTO/LAO structures are distinguished by the lowest dielectric losses ($\tan\delta < 9 \times 10^{-4}$) and $T_m < 230$ K. However, BSTO/MgO structures show very little capacitance tunability T. The BSTO/α structures are characterized by stronger lattice mismatch and structural distortions than the BSTO/LAO system. This feature gives rise to textured or polycrystalline phase in the FEF characterized by $\chi_0 > 0.8$. The BSTO/α samples have $\tan\delta > 1.5 \times 10^{-3}$ and $T_m > 260$ K. Thus, the dielectric properties of BSTO films and the T_m value are strongly dependent on distortions of their crystal structure. The most appropriate from the point of view of radioelectronics, combination, including low dielectric losses of BSTO films, high tunability factor and minimum deviation of T_m, is observed for the BSTO/α structures.

References

[1] Lancaster M J, Powell J and Porch A 1998 *Supercond. Sci. Technol.* **11** 1323–34

[2] Van Keuls F W, Romanofsky R R, Bohman D J, Winters M D, Miranda F A, Mueller C H, Treece R E, Rivkin T V and Galt D 1997 *Appl. Phys. Lett.* **71** 3075–8

[3] Vendik O G, Ter-Martirosyan L T, Dedyk A I, Karmanenko S F and Chakalov R A 1993 *Ferroelectrics* **144** 33–43

[4] Vendik O G and Ter-Martirosyan L T 2000 *J. Appl. Phys.* **87** 1435–9

[5] Vendik O G and Zubko S P 2000 *J. Appl. Phys.* **88** 5343–40

[6] 1982 *Acoustic crystals* ed M P Shaskol'skaja (Moscow: Nauka) (In Russian)

[7] Karmanenko S F, Dedyk A I, Isakov N N, Ter-Martirosyan L T, Semenov A A, Gordeichuk A V and Hagberg J 2001 *Techn. Phys.* **46** 482–502

[8] Afrosimov V V, Dzjuba G O, Il'in R N, Panov M P, Sakharov V I, Serenkov I T and Ganza E A 1996 *Techn. Phys.* **41** 1240–6

[9] Karmanenko S F, Belousov M V, Davydov V Yu, Vendik O G, Likholetov Yu V, Chakalov R A, Kozyrev A B, Serenkov I T and Il'in R N 1993 *Supercond. Sci. Technol.* **6** 23–9

[10] Feldman L C, Mayer J W and Picraux S T 1982 *Material Analysis by Ion Channeling* (New York: Academic Press) p 300

[11] Afrosimov V V, Il'in R N, Karmanenko S F, Panov M N, Sakharov V I and Serenkov I T 1997 *Poverkhnost'* **8** 71–5

[12] Kim W J, Chang W, Qadri S B, Pond J M, Kirchoefer S W, Chrisey D B and Horwitz J S 2000 *Appl. Phys. Lett.* **76** 1185–7